Supplementary Figures:

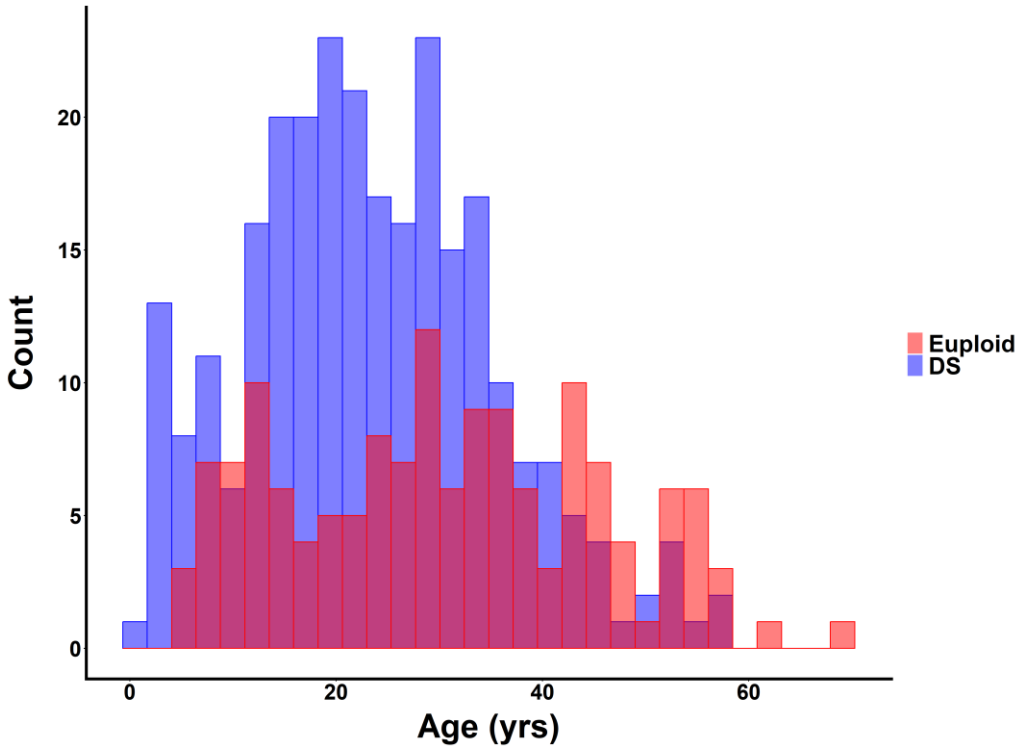

Supplementary Figure 1: Age distribution histograms of 270 DS in blue (127 female and 143 male) and 146 euploid individuals in red (83 female and 63 male). The age range of DS individuals was between 0.5 and 56.7 years (mean: 23.44) and that of euploid was between 4.2 and 69.1 years (mean: 30.46).

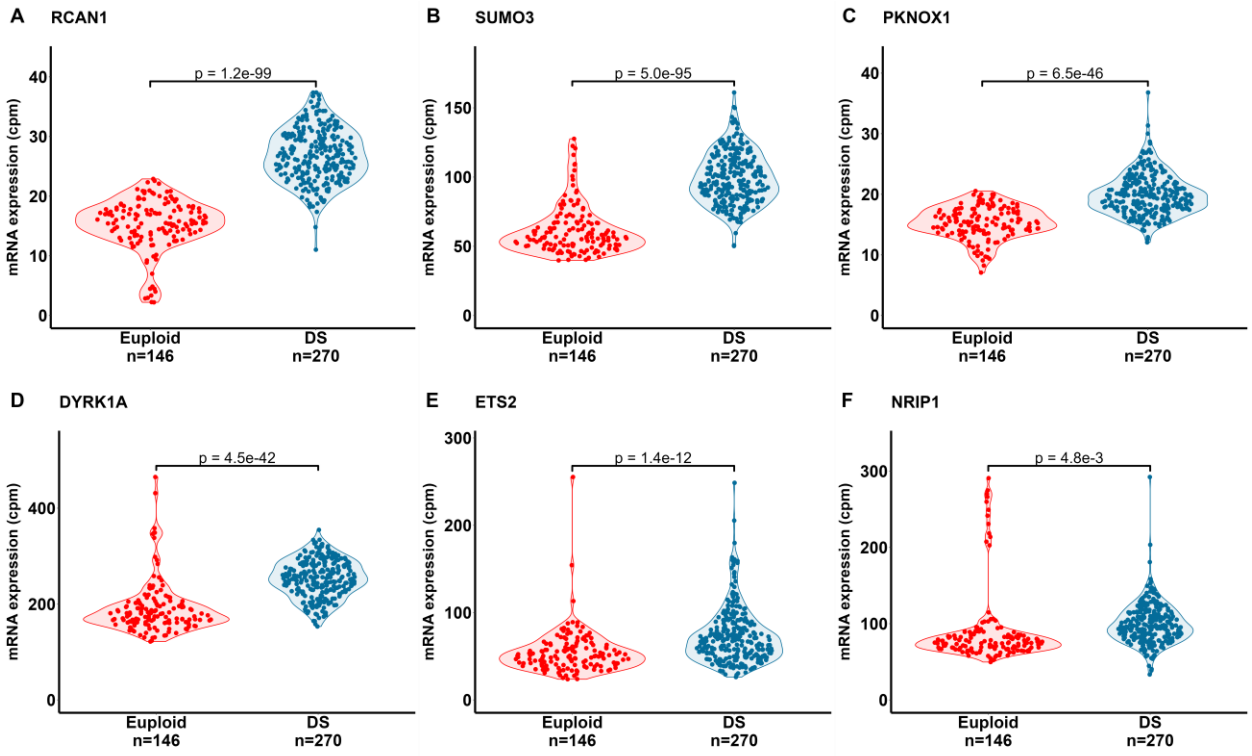

Supplementary Figure 2: Increased expression of Ch. 21 genes for which a dosage imbalance is implicated in dysregulated mitochondrial biogenesis and function[1,2] including a.) *RCAN1*, b.) *SUMO3*, c.) *PKNOX1/PREP1*, d.) *DYRK1A*, e.) *ETS2*, f.) *NRIP1*. Likelihood-ratio test, edgeR.

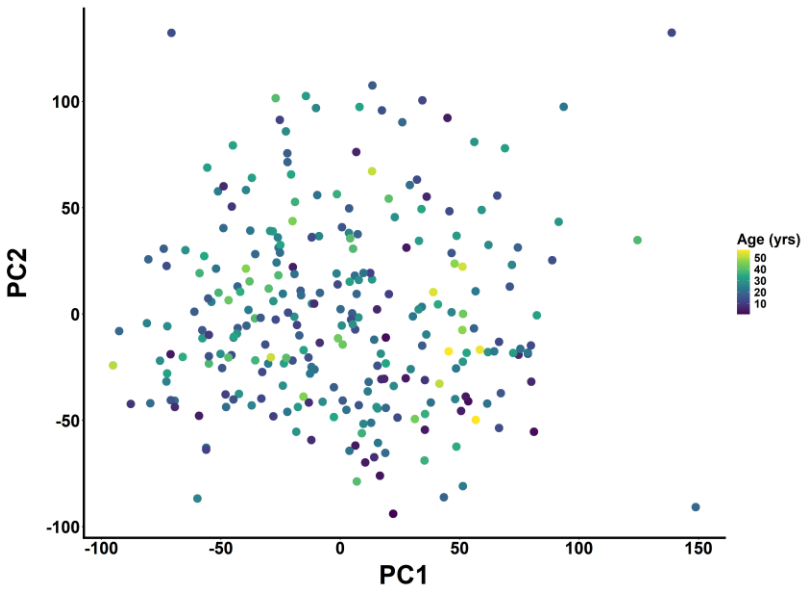

Supplementary Figure 3: Principal Component Analysis (PCA) of DS individuals (n = 270) by whole transcriptome mRNA expression. Dots represent individuals. Coloring by age reveals no qualitative clustering of individuals.

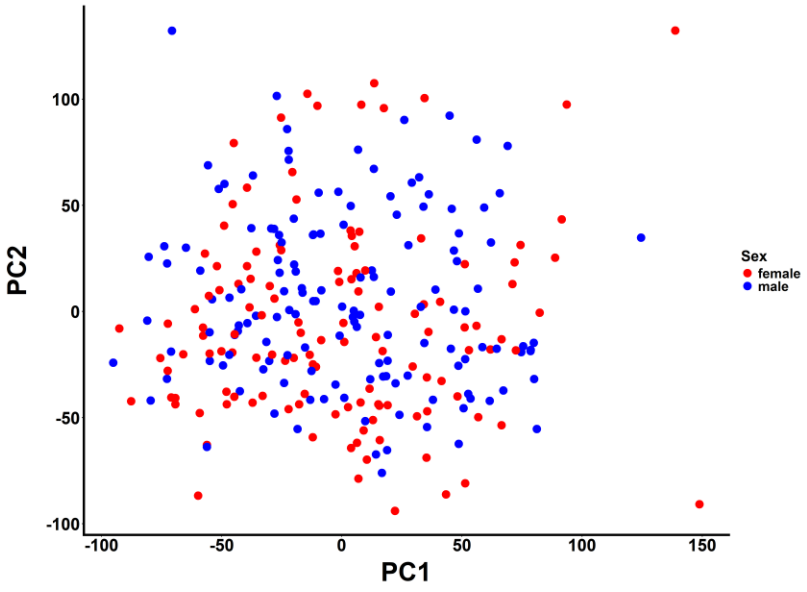

Supplementary Figure 4: PCA of DS individuals (n = 270) by whole transcriptome mRNA expression. Dots represent individuals. Coloring by sex reveals no qualitative clustering.

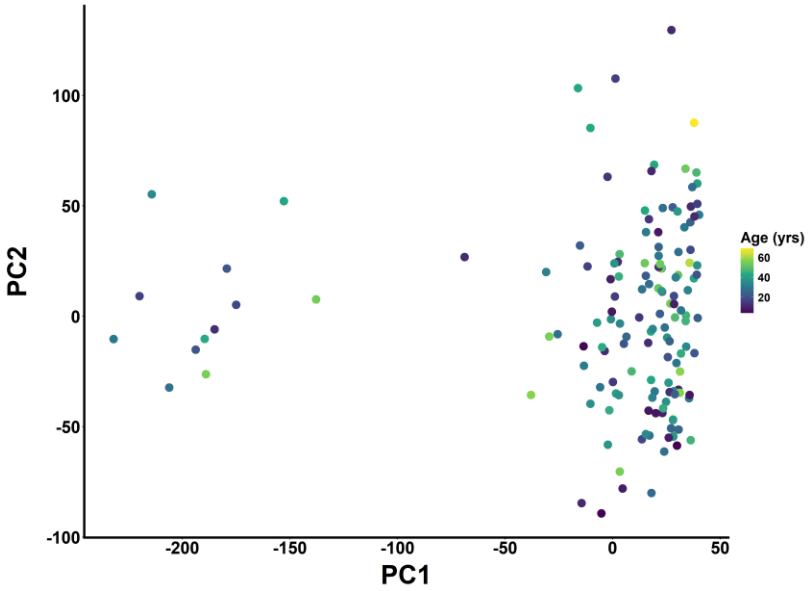

Supplementary Figure 5: Principal Component Analysis (PCA) of euploid individuals (n = 146) by whole transcriptome mRNA expression. Dots represent individuals. Coloring by age reveals no qualitative clustering of individuals.

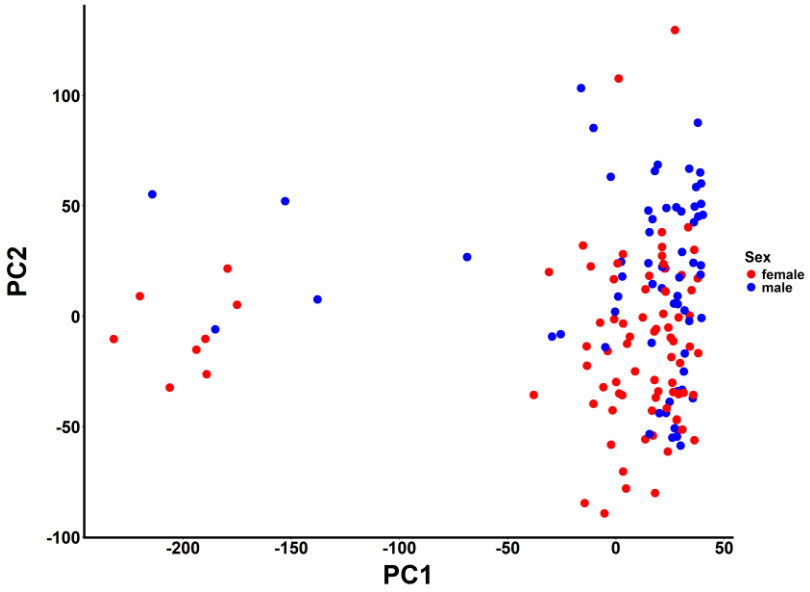

Supplementary Figure 6: PCA of euploid individuals (n = 146) by whole transcriptome mRNA expression. Dots represent individuals. Coloring by sex reveals no qualitative clustering.

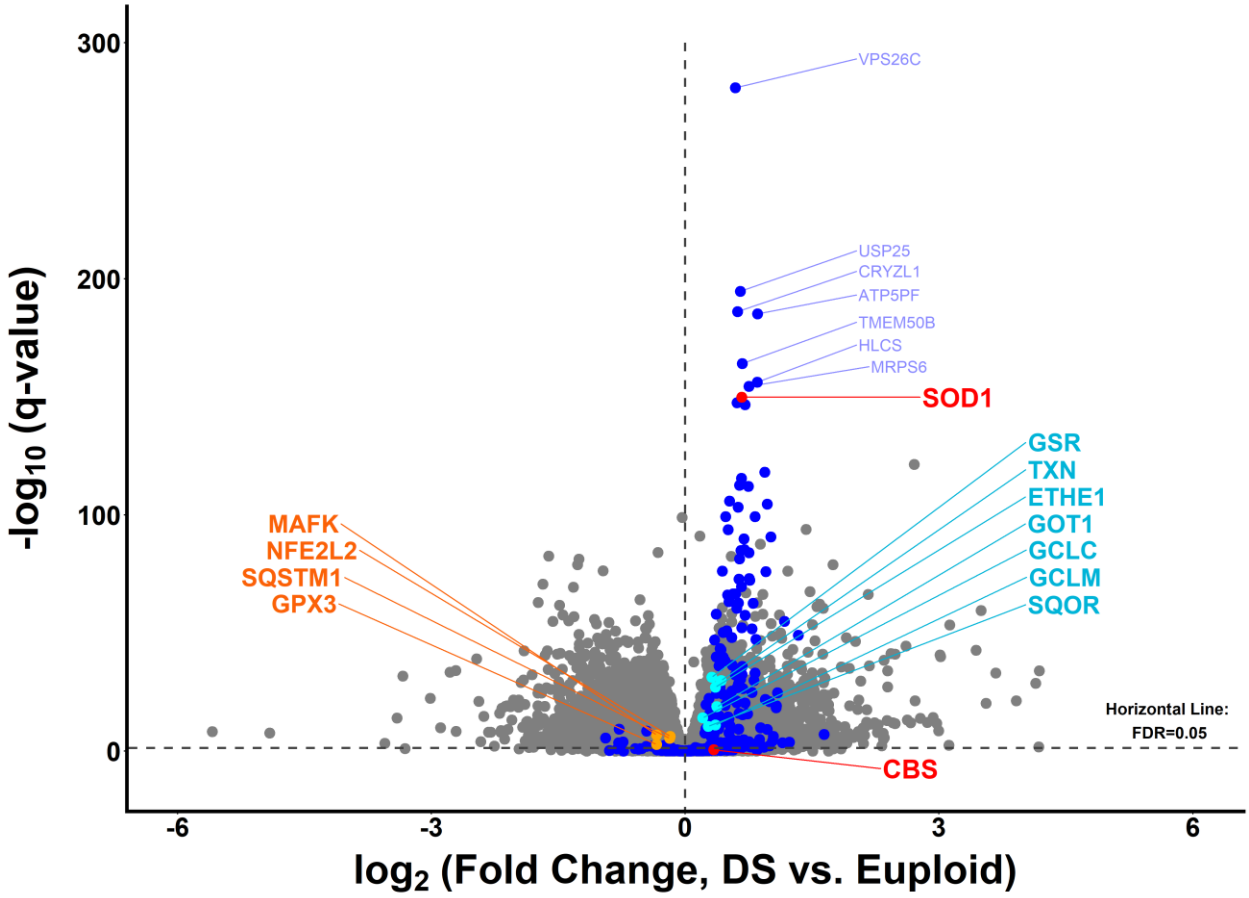

Supplementary Figure 7: Genes with differentially higher and lower expression in DS relative to euploid, accounting for age- and sex effects. Dots represent individual genes, with Hsa21 genes colored in blue. Significantly higher expression of *SOD1*, but not *CBS* in DS WBCs relative to euploid individuals. Key non-Ch.21 genes involved in antioxidant homeostasis and sulfide metabolism whose expression was previously noted as significantly higher in DS (**Figures 6 and 8;** *GSR, TXN, ETHE1, GOT1, GCLC, GCLM, SQOR*) remained so (colored in cyan), as did non-Ch. 21 genes identified as significantly lower in DS (colored in orange) with the reduced model (**Figure 6**; *MAFK, NFE2L2, SQSTM1, GPX3).* Gene expression fold changes calculated from comparisons between DS and euploid individuals using edgeR, with age and sex as fixed-effect covariate predictors. Q-values were calculated from p-values following correction for multiple comparisons using the Benjamini-Hochberg method.

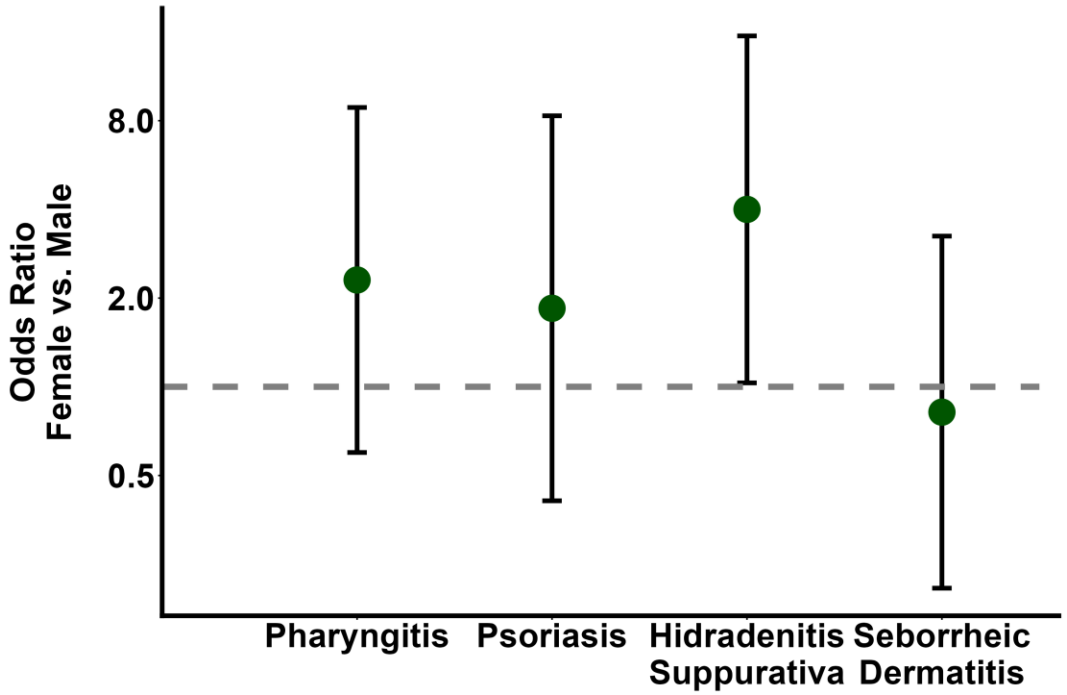

Supplementary Figure 8: Odds ratios of selected conditions in DS females versus males, account for *SOD1* expression status and age. Higher odds of pharyngitis, psoriasis and hidradenitis suppurativa, albeit non-significant.

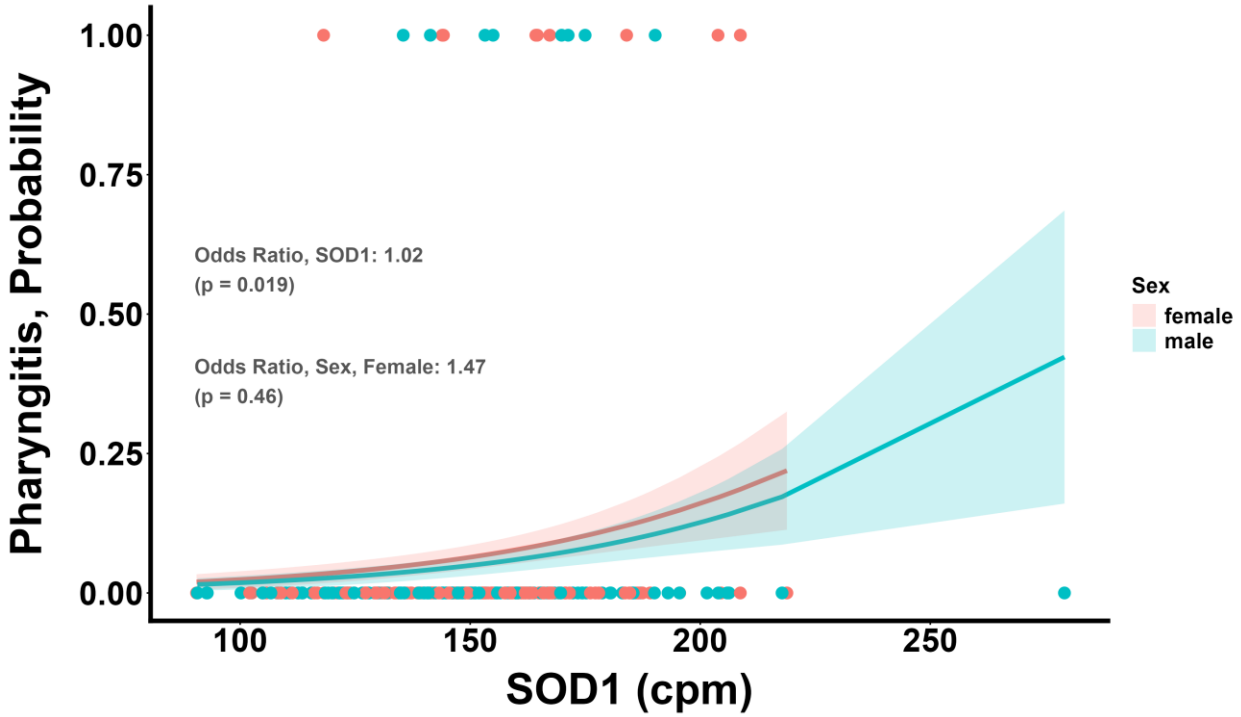

Supplementary Figure 9: Continuous predictor binomial logistic regression model of pharyngitis probability as a function of *SOD1* expression across DS individuals (n=270). Dots represent individuals, colored by sex. A probability of 1 was assigned to individuals with pharyngitis. In both female and male DS individuals, the probability of pharyngitis as a co-occurring condition significantly increased with higher *SOD1* mRNA expression. The effect of sex on pharyngitis probability was not statistically significant. Wald Z-test.

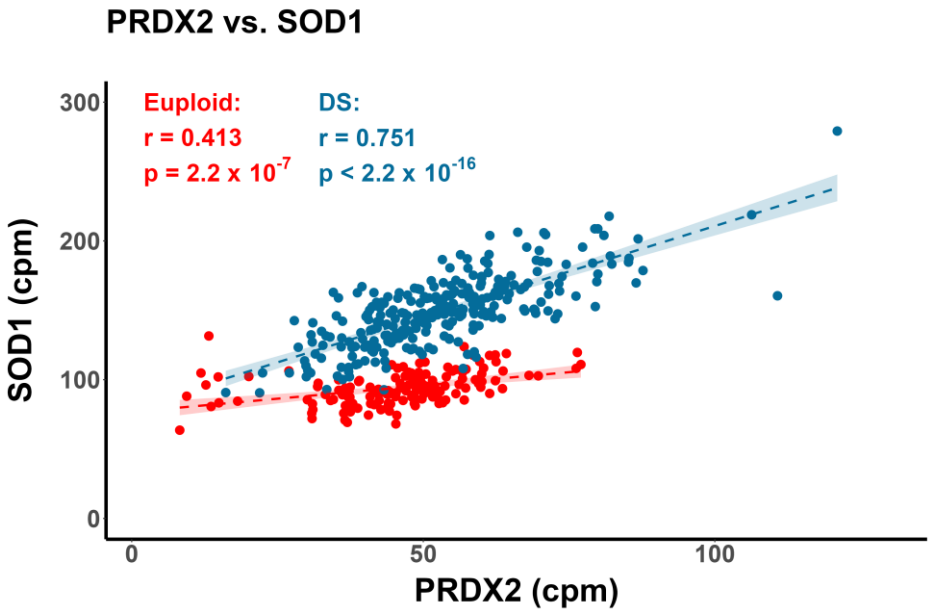

Supplementary Figure 10: *SOD1* and *PRDX2* positively correlated in euploid and DS individuals, represented by dots (n= 146 and 270 respectively). Pearson's r, linear regression t-test.

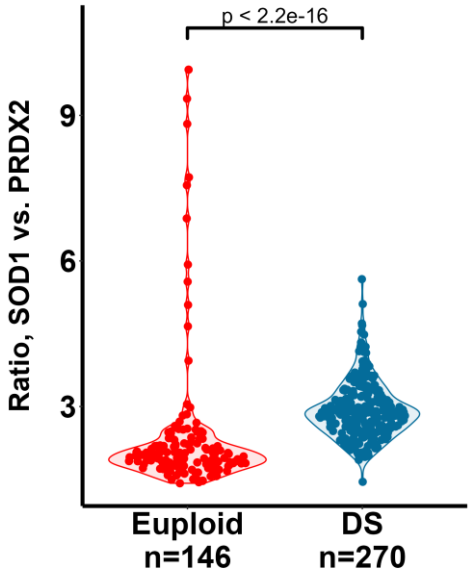

Supplementary Figure 11: Higher *SOD1/PRDX2* mRNA expression ratios in DS individuals relative to euploid. Each dot represents 1 individual. Mann-Whitney U-Test.

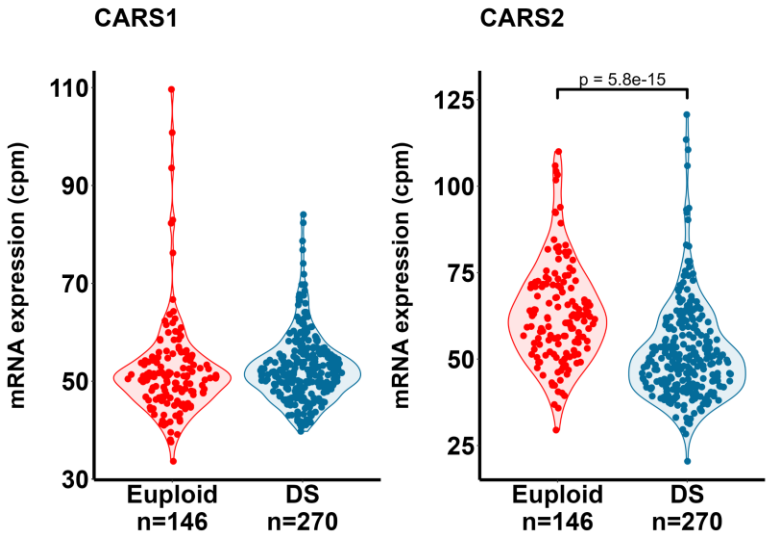

Supplementary Figure 12: Similar *CARS1* and lower *CARS2* mRNA expression in DS individuals relative to euploid. Each dot represents 1 individual. Likelihood-ratio test, *edgeR*.

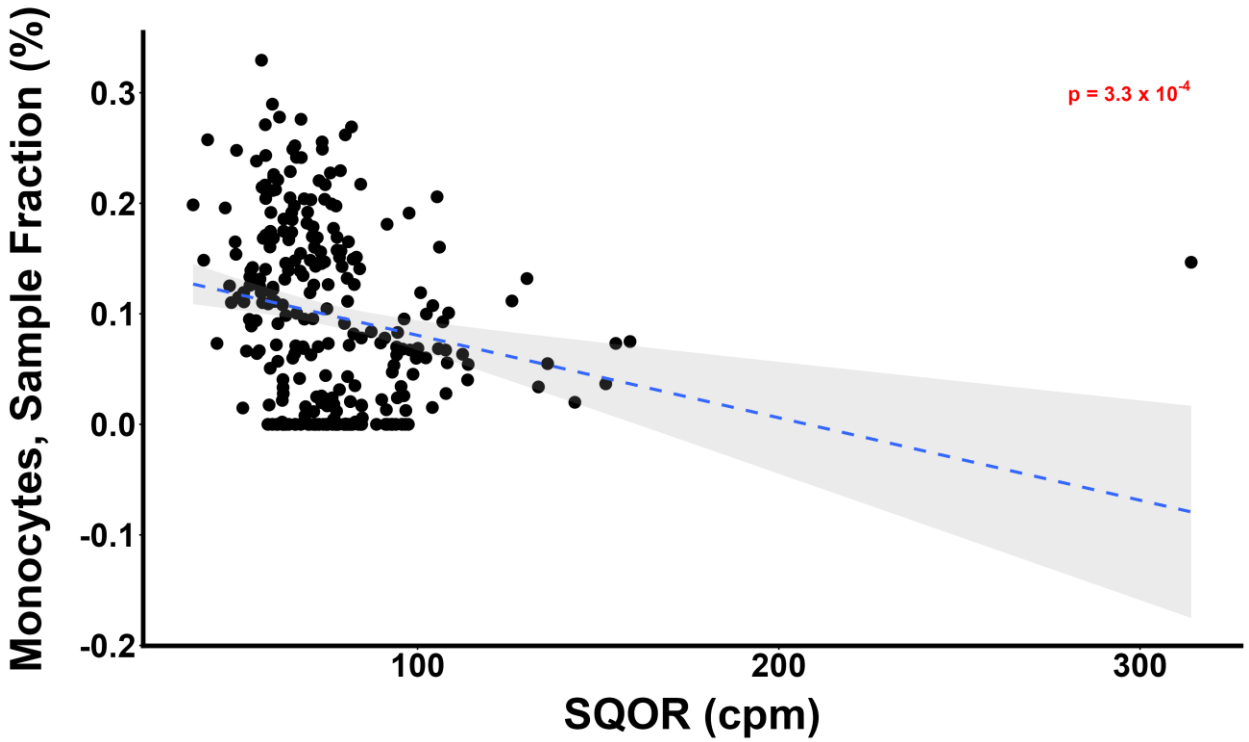

Supplementary Figure 13: Continuous predictor model of imputed monocyte fraction in DS individuals (n = 270; dots) as a function of *SQOR* mRNA expression. Significant decrease in monocyte fraction with increasing *SQOR* expression. Dashed line indicates regression model, with standard error of slope as a shaded region.Pearson's r.

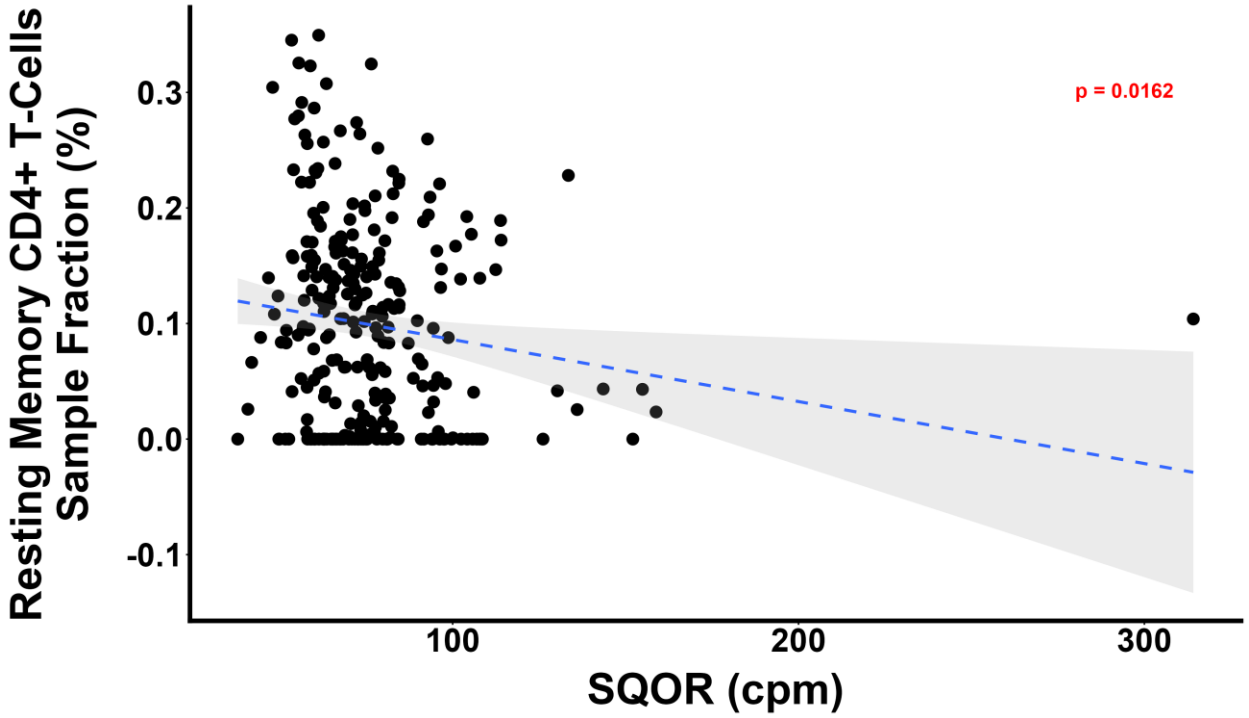

Supplementary Figure 14: Continuous predictor model of imputed resting memory CD4+ T-cell fraction in DS individuals (n = 270; dots) as a function of *SQOR* mRNA expression. Significant decrease in resting memory CD4+ T-cell fraction with increasing *SQOR* expression. Dashed line indicates regression model, with standard error of slope as a shaded region. Pearson's r.

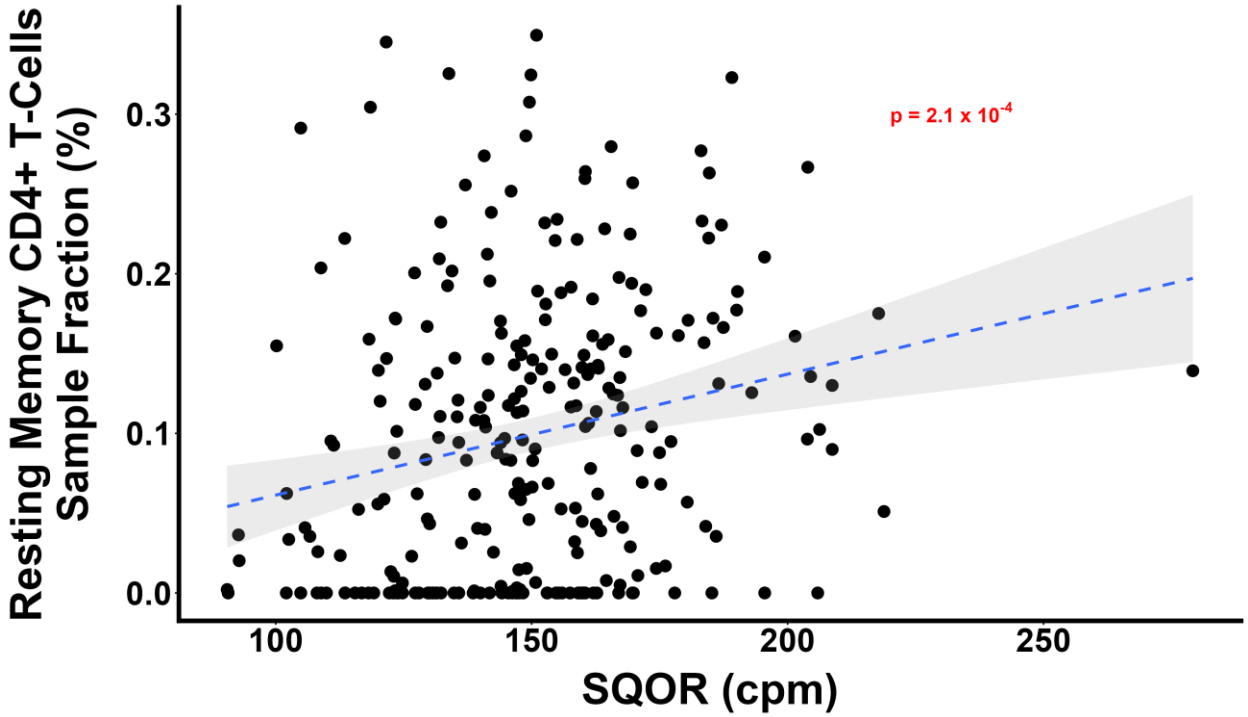

Supplementary Figure 15: Continuous predictor model of imputed resting memory CD4+ T-cell fraction in DS individuals (n = 270; dots) as a function of *SOD1* mRNA expression. Significant increase in resting memory CD4+ T-cell fraction with increasing *SOD1* expression. Dashed line indicates regression model, with standard error of slope as a shaded region. Pearson's r.

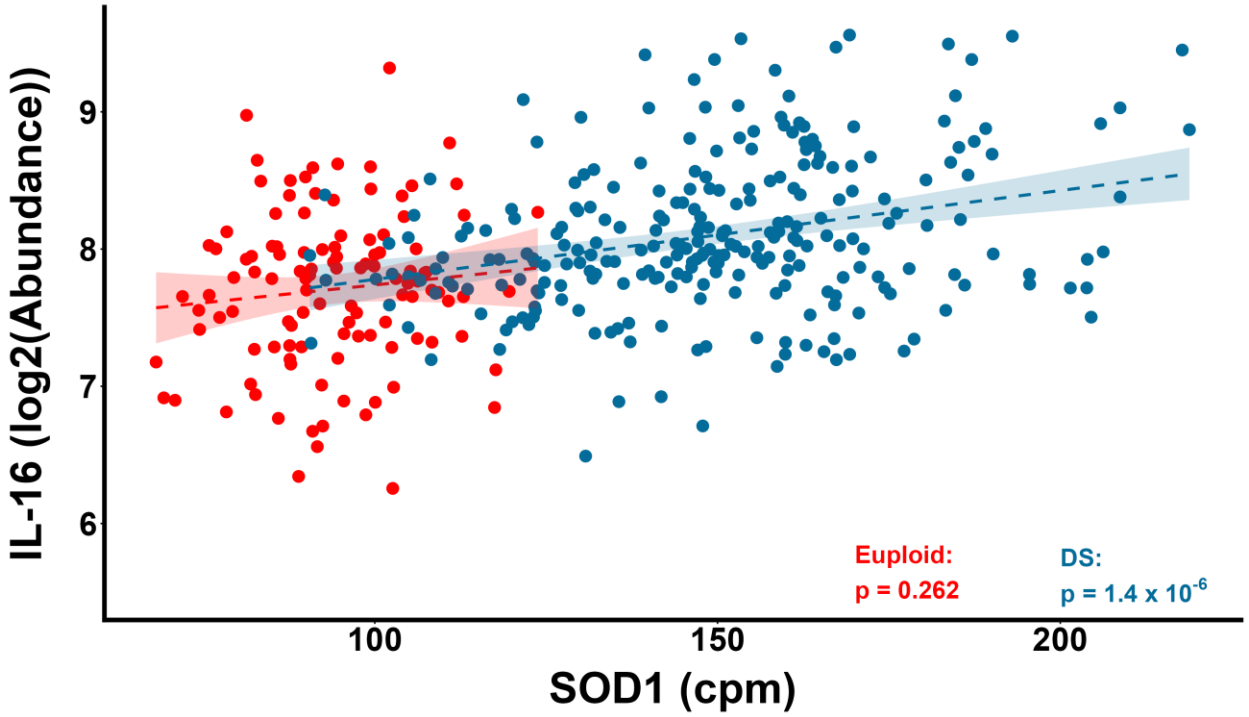

Supplementary Figure 16: Continuous predictor model of IL-16 log2-transformed abundance in DS (n = 270; dots) and euploid (n = 146; dots) as a function of *SOD1* mRNA expression. Significant increase in DS IL-16 with increasing *SOD1* expression. Dashed line indicates regression model, with standard error of slope as a shaded region. Pearson's r.

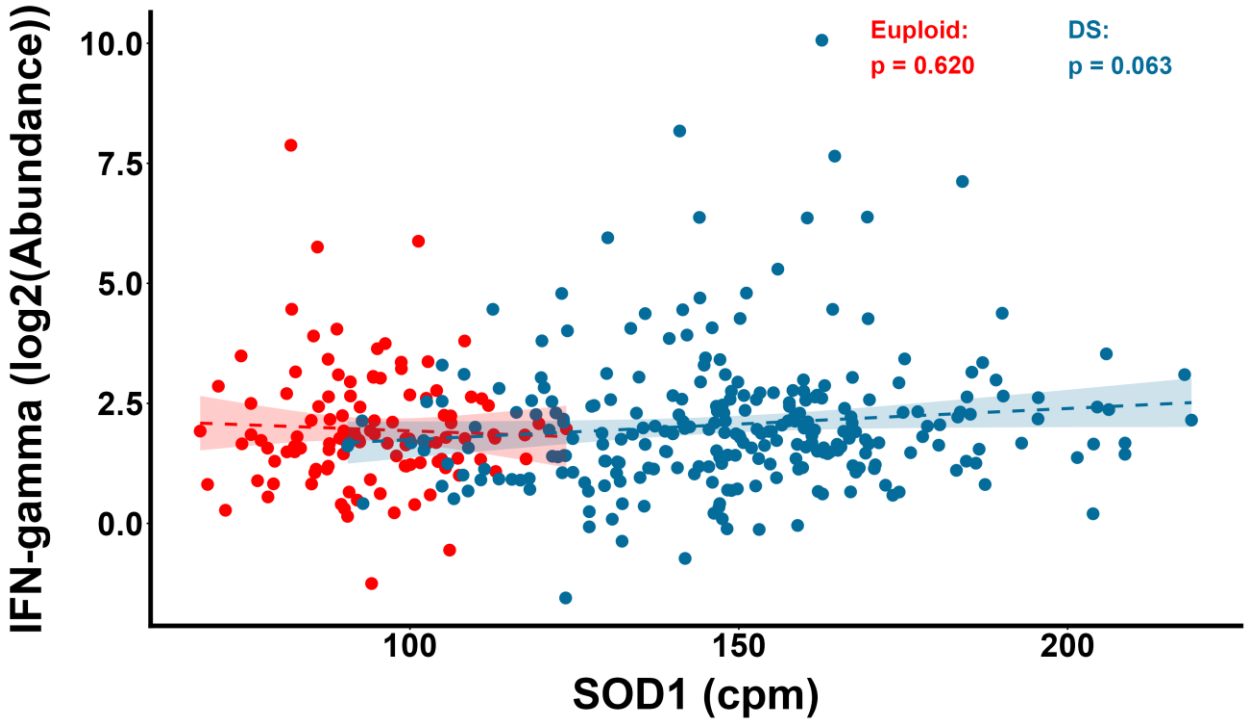

Supplementary Figure 17: Continuous predictor model of IFN-γ log2-transformed abundance in DS (n = 270; dots) and euploid (n = 146; dots) as a function of *SOD1* mRNA expression. Trend toward increase in DS IFN-γ with increasing *SOD1* expression. Dashed line indicates regression model, with standard error of slope as a shaded region. Pearson's r.

References:

1 Izzo, A. *et al.* Mitochondrial dysfunction in down syndrome: molecular mechanisms and therapeutic targets. *Molecular Medicine* **24**, 2, doi:10.1186/s10020-018-0004-y (2018).

2 Vilardell, M. *et al.* Meta-analysis of heterogeneous Down Syndrome data reveals consistent genome-wide dosage effects related to neurological processes. *BMC Genomics* **12**, 229, doi:10.1186/1471-2164-12-229 (2011).